JOURNAL OF MATERIALS SCIENCE 37 (2002) 4109–4115

Diacid architecture effect on the synthesis and microstructure of rigid-rod poly(benzobisimidazoles)

C. C. CHEN
Institute of Materials Science & Engineering, National Sun Yat-Sen University, Kaohsiung 804, Taiwan

L. F. WANG*, J. J. WANG
Department of Chemistry, Kaohsiung Medical University, Kaohsiung 807, Taiwan

T. C. HSU*, C. F. CHEN
Institute of Materials Science & Engineering, National Sun Yat-Sen University, Kaohsiung 804, Taiwan
E-mail: tjhsu@mail.nsysu.edu.tw

Six poly(benzobisimidazoles) (PBIs) have been synthesized by the solution polycondensation of 1,2,4,5-tetraaminobenzene tetrahydrochloride in poly(phosphoric acid) (PPA) with systematically varied diacids to demonstrate the solubilization of the aromatic heterocyclic rigid-rod polymers. The role of PPA is identified and the effects of phosphorous pentoxide and water on PBI during polycondensation are discussed. Polymer properties such as the inherent viscosity, decomposition temperature are correlated to the polymer concentration. Finally, the effect of diacid architecture on the synthesis and microstructure of PBI is studied. The results are further discussed in terms of resonance, symmetry, and solubilization of the diacids.

1. Introduction

The conjugated rigid-rod aromatic heterocyclic benzazo polymers, generally referred as PBX, have attracted much attention in both academic and industrial communities [1–3]. While original motivation of PBX concentrated on the development of mechanical, thermal, and oxidative stability [4, 5], current interests have shifted to the tremendous potentials in the optical and electrical applications such as third-order nonlinear optical (NLO) materials or polymer electrolytes used in secondary lithiumion battery [6–15]. Historical development of PBX starts in 1961 from synthesis and processing of poly(benzobisimidazole) (PBI); yet, major advances in the last two decades have been centered on poly(benzobisthiazole) (PBT) and poly(benzobisoxazole) (PBO). In particular, fibers, films, or molecular composites of PBT and PBO have been commercially perceived [16–19].

PBI can be prepared directly by means of polycondensation of 1,2,4,5-tetraaminobenzene tetrahydrochloride with certain diacids in poly(phosphoric acid) [20, 21]. However, they are generally insoluble in common organic solvents, rendering themselves limited potential utilities in spite of many targeted applications. Methods to improve the solubility of aromatic heterocyclic rigid-rod polymers have been proposed. The complex formation with Lewis acids in aprotic organic solvents is a successful approach [22, 23]; it is extremely suitable for thin film applications but is less thermally stable due to residual Lewis acid in the film. A novel two-step synthesis via polyamide precursor to prepare PBT was proposed [24–26]. This method utilizes the better solubility of polyamides to improve the processing difficulty; the precursor is then converted to PBTs via thermal cyclization. Incorporation of flexible diacid monomers into the main chain of PBT to form either random or block copolymers is another efficient way suggested [18]. This idea was extended to incorporate soluble pendant group onto diacids of the rigid-rod polymers; the alkyl or the sulfone pendant groups were two groups frequently referred [10,11,13]. Another coagulation processing scheme was developed for NLO thin films [27–29]. An optically isotropic polymer solution was rapidly frozen to preserve molecular dispersion of polymer in the solvent; it was then coagulated cryogenically without disrupting the molecular distribution. Finally, chemical modifications with organic-soluble dopants on the final aromatic heterocyclic polymers was also mentioned, i.e., the sulfonated PBIs [11].

Most of the above efforts have been directed toward PBTs and PBOs, with relatively few interests in PBIs. To further explore the solubilization of PBIs and the accompanied problems, the present paper deals with a diacid architecture effect on the microstructure, thermal

*Authors to whom all correspondence should be addressed.

and optical properties of PBIs. Six PBIs with different degree of flexibility of diacids in the main chain have been synthesized. The diacids used include terephthalic acid, 2,6-napthalene dicarboxylic acid, 4,4'-biphenyl dicarboxylic acid, 2,2'-biphenyl dicarboxylic acid, 4,4'-oxybis(benzoic acid), and 4,4'-sulfonyl bis(benzoic acid). The chemical structure of the diacids were varied mainly in the main chain of PBIs, different from those reported on side chain variation of PBI [11, 13] or on main chain variation of PBT [3, 9]. The results were discussed in terms of conjugation, symmetry, and electrophilicity of the diacids in detail.

2. Experimental

2.1. Materials

1,2,4,5-tetraaminobenzene tetrahydrochloride (TABTC, Fluka Chemicals) was used as received to react with the following acids: terephthalic acid (1, Riedel-de Haen). 2,6-naphthalene dicarboxylic acid (2, Aldrich), 4,4'-biphenyl dicarboxylic acid (3, Aldrich), and 2,2'-biphenyl dicarboxylic acid (4, Aldrich), 4,4'-oxybis(benzoic acid) (5, TCI), and 4,4'-sulfonyl bis(benzoic acid) (6, TCI). Chemical structures of the diacids are depicted in Scheme I, along with the polycondensation reaction. Phosphorous pentoxide (P_2O_5) was obtained from Acros. 85% phosphoric acid (H_3PO_4, Tedia) and 83% poly(phosphoric acid) (PPA, from TCI) were used as received to prepare 77% fresh PPA used in the dehydrochlorination of TABTC. PPA was prepared at 150°C for 6 h under argon atmosphere with a weight ratio of H_3PO_4: P_2O_5 = 1 : 1.52. The following solvents were used in this study: methanesulfonic acid (MSA, TCI), dimethyl sulfoxide (DMSO, Merck), and trifloroacetic acid (TFAA, 99%, Aldrich), dichloromethane (DCM, Tedia).

2.2. Polycondensation

PBIs were prepared according to the reported method [2]. It is described in brief here to emphasize the materials and processing parameters used. TABTC was dissolved in deaerated 77% PPA under nitrogen atmosphere with mechanical stirring at room temperature for 24 h. After dehydrochlorination at 65°C for 24 h under vacuum, equimolar amount of diacid was added together with appropriately adjustable amount of P_2O_5 to control the water content in the final solution. Unless otherwise indicated, the polymer concentration was 1.1 wt% and the polycondensation temperature was 165°C for 8 h, then 185°C for 8 h, and finally 200°C for 48 h. The corresponding polymers synthesized using the diacids depicted in Scheme I are abbreviated as PBI-1 to PBI-6. The polymerization dope in PPA was washed and precipitated in deionized water. The synthesized PBIs were further purified by Soxhlet extraction for 72 h to completely remove PPA and also the residual TABTC and diacid monomers. It was then dried in a vacuum oven at 65°C for 48 h.

2.3. Preparation of thin films

To prepare thin films of PBIs, the polymerization dope was first dissolved in MSA, cast onto a glass plate to form a thin film, then was extracted in water for typically 2–3 days to free the film of acid. After evaporation of MSA, it was washed with basic organic solvent MeOH and dried in a vacuum oven at 65°C for 48 h.

2.4. Characterization

Inherent viscosity η_{inh} of the PBIs were measured with a concentration of 3.0 kg/m^3 (or 0.3 g/dL) in methanesulfonic acid at 30°C using a Cannon Ubbelohde capillary viscometer. FTIR spectra were recorded (Bio-Rad FTS-40 spectrophotometer, Perkin Elmer 2000) with a resolution of 4 cm^{-1}, scanning from 4000–400 cm^{-1}. PBI thin films were measured directly, while powders of PBIs were mixed with KBr as thin pellets and measured. Thermogravimetric analysis (TGA) was carried out with a Perkin-Elmer TGA-7 thermogravimetric analyzer, scanning from 50–800°C with a scanning rate 10°C/min. X-ray powder diffraction, crystalline phase and growth directions were determined by XRD (Siemens D5000, Karlsruhe, Germany) with

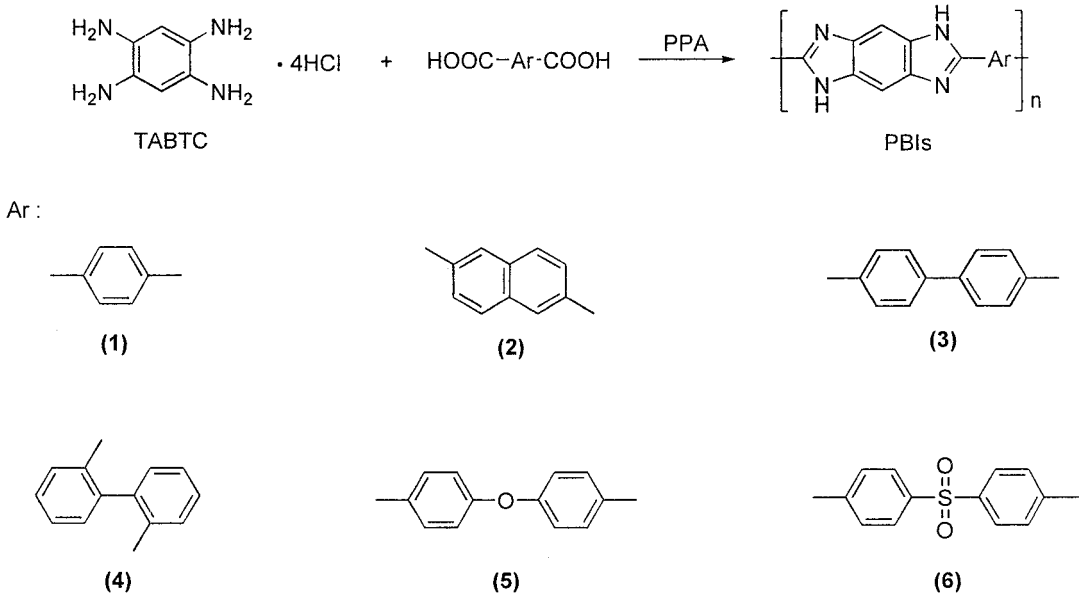

Scheme I Chemical structure of diacids and the polycondensation.

Cu K_α radiation operated at 40 KV and 30 mA. The 2θ scan range was set to be 4–80° using a step scan of 0.05°/sec. Optical UV-visible absorption spectra of PBIs in MSA were obtained (Simadzu UV-160A spectrophotometer) in the wavelength range of 190–600 nm. Finally, the solubility of the polymers was evaluated using a number of organic solvents, mainly, strong acids. The neat polymers were exposed to solvents at room temperature. Solubility was inferred from the degree of dissolution of polymer in the dilute region.

3. Results and discussion

3.1. Role of PPA and phosphorous pentoxide

To maintain the effectiveness of PPA is the key to a successful polycondensation of PBIs. The PPA acts, in the first place, as a solvent to dissolve the monomers. Once dissolved, PPA then is responsible for the dehydrochlorination of the monomer TABTC before polycondensation proceeds. Meanwhile, additional P_2O_5 is needed to compensate for the condensation by-product water. At the end of polymerization, the P_2O_5 content must be >82% for a production of high molecular weight. η_{inh} of PBI-1 without P_2O_5 addition is less than half of the PBI with the regular P_2O_5 dose (30%) and also the decomposition temperature T_d as measured by TGA is 42°C less (Table I). T_d is defined as the temperature at which a 10% weight loss was recorded; whereas the char yield indicates the residual weight in % when heated to 800°C in nitrogen. This suggests that incomplete dehydration due to absence of P_2O_5 allows water molecules to reside in the PBI-1 sample, resulting in a poor thermal stability and a reduced molecular weight. On the other hand, a considerable reduction of 89°C in T_d (Table I) for the sample with extra P_2O_5 is found. In this circumstance, polycondensation in the very viscous solution is greatly hindered and the excess P_2O_5 (60%) is difficult to be removed from the system.

3.2. Effect of polymer concentration

The final polymer concentration C, in weight% of the total weight of the solution S, is defined [1] as $C = Y/S$, where Y is the theoretical polymer yield in gram based on the quantity of added monomers. The solution S includes polymer Y, PPA, the added P_2O_5, and the water of the polycondensation by-product (all in gram). Note that 4 moles of H_2O are produced when one mole of repeated unit formed in the condensation. According to the above definition, the effect of polymer concentration may be regarded as the effect of PPA or P_2O_5 concentration.

TABLE I Effect of P_2O_5 concentration for sample PBI-1

P_2O_5 (%)[a]	P_1[b] (%)	P_2[b] (%)	P_3[b] (%)	η_{inh} (dL/g)	T_d (°C)
0	84.9	84.9	84.9	1.15	660
30[c]	84.9	88.3	88.0	2.89	702
60	84.9	90.4	90.0	2.73	613

[a]wt% of added P_2O_5 to PPA before polycondensation.
[b] P_1 is wt% of P_2O_5 in the original PPA; P_2 is wt% of P_2O_5 added before polycondensation; and P_3 is wt% of P_2O_5 after polycondensation. Refer to Ref. [1] for detailed definition.
[c]Regular dose of P_2O_5 in a typical PBI polycondensation.

TABLE II Effect of polymer concentration for sample PBI-1

PBI conc.(%)	η_{inh} (dL/g)	T_d (°C)	2θ (degree)	d-spacing (nm)
4.3	0.95	613	10.715	0.825
			26.242	0.339
2.2	1.73	576	12.243	0.722
			26.264	0.339
1.1	2.89	582	11.456	0.771
			26.490	0.336

Duration of polycondensation at 200°C was 24 h.

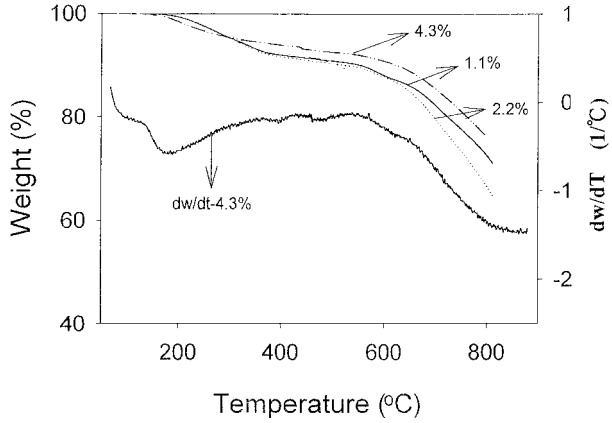

Figure 1 Effect of polymer concentration on the thermal stability of PBI-1.

The viscosity data listed in Table II indicate that η_{inh} increases almost linearly with the decreased polymer concentration. On the other hand, similar thermal behavior is found in Fig. 1 as indicated by small fluctuation among the three PBIs. The accompanied derivative curve in Fig. 1 for the sample with $C = 4.3\%$ reveals a multi-staged decomposition behavior. In a diluted reaction mixture, the monomers are easier to dissolve in PPA and so is the dehydrochlorination of DABTC, both effects are in favor of subsequent polycondensation, resulting in a PBI with high a η_{inh}; also, water is readily removed by the nearby abundant P_2O_5 once it is produced as a condensation by-product. Polycondensation is very sensitive to water and will be hindered in a reaction system with high polymer concentration.

The XRD results summarized in Table II reveal that in general, there are two major peaks for a typical PBI. Take PBI-1 sample with $C = 1.1$ wt% as an example, the (200) peak at $2\theta = 11.456°$ is assigned to the side-to-side packing and the (010) peak at $2\theta = 26.490°$ is assigned to the face-to-face packing, consistent with the previously reported data for PBT [30, 31]. This corresponds to a = 1.542 nm and b = 0.336 nm in a non-primitive monoclinic unit cell. A schematic representation is given in Fig. 2 to illustrate the molecular structure of PBI-1. One may note that the d-spacing in the b-direction is only about one quarter of that in the a-direction. It appears that all the three samples exhibit characteristic (200) and (010) peaks, suggesting molecular packing of PBI-1 is not affected substantially by the polymer concentration, Generally speaking, the

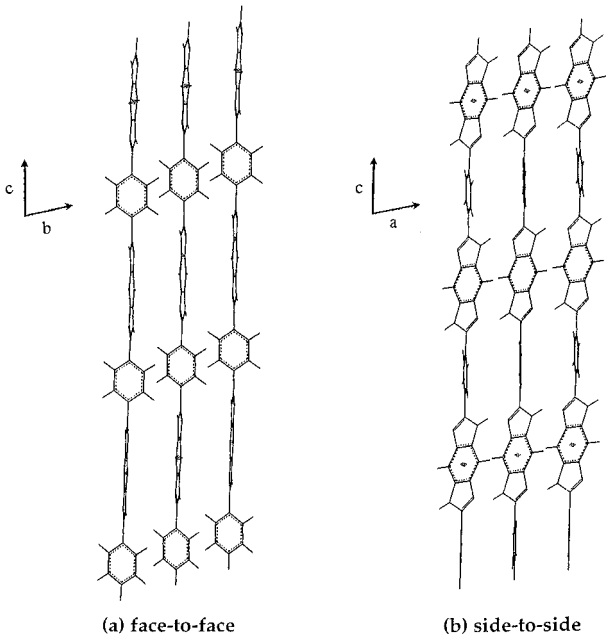

Figure 2 Schematic diagram showing the face-to-face (a) and side-to-side (b) packing of PBI-1.

(200) peak moves to higher diffraction angle as polymer concentration is reduced; this means an increased *d*-spacing along the side-to-side direction. Clearly, the lower polymer concentration allows the monomers to be more freely diffused and reacted, and a more compact microstructure can be formed.

3.3. Resonance effect

Comparison is made among PBI-1, 2, and 3 to illustrate the resonance effect of diacid monomers. It is expected the naphthalenyl unit (PBI-2) is more conjugated and coplanar than the benzyl unit (PBI-1). The biphenyl unit (PBI-3), with the free rotation of C–C bond between the two benzene rings is the least among the three PBIs. η_{inh} listed in Table III indicates that the absolute molecular weight of PBI-1 is far higher than all the others. Substitution of benzyl with naphthalenyl or biphenyl in diacid greatly reduced η_{inh} (~1/3 less) of PBIs. In general, η_{inh} of all the PBIs synthesized in this study, although lower than PBT or PBO, was in the right range as reported [3].

FTIR spectra of PBIs are given in Fig. 3. Several characteristic bands of PBI can be observed such as the out-of-plane heteroring deformation at ~693 cm^{-1} (P1), the heteroring breathing at ~952 cm^{-1} (P4), the benzene ring 1,2,4,5-C_6H_4- at 1009 cm^{-1} (P5), the C–C stretching at 1234 cm^{-1} (P6) and the heteroring stretching at ~1366 cm^{-1} (P7) of PBI-1. The heteroring stretching associated with the imidazole ring can also be clearly identified by the strong C=N band at 1607 cm^{-1} (P8). On the other hand, band associated with the diacid portion can be identified at 836 cm^{-1} (P2) for C_6H_4-ring or 886 cm^{-1} (P3) for C_6H_3-ring. Additional peaks at 1164 cm^{-1} (P9) and 1151 cm^{-1} (P10) are assigned to the ether linkage of PBI-5 and sulfone linkage of PBI-6, respectively. In essence, the FTIR spectra are consistent with previous reports on PBT series [6]. The frequency of the out-of-plane heteroring deformation at ~693 cm^{-1} of PBI-1 is shifted in PBI-2 (Table III) to 706 cm^{-1}; the C=N band and the C_6H_4 ring stretching (in fact, C_6H_4) appear at 1620 cm^{-1} and 895 cm^{-1}, respectively. This represents an increase in frequency (or in force constant) of this resonance vibration motion due completely to the substitution of benzene ring by naphthalene ring.

The weight loss vs. temperature of the PBIs by TGA is plotted in Fig. 4. For a typical rigid-rod PBI, T_d as high as 708°C and char yield ~85% are attainable (PBI-1 to 3, Table III). Worthy of note is that there is no direct relation between the thermal stability and the viscosity. From the thermal stability point of view, there is insignificant difference among the benzyl, naphthalenyl, and biphenyl unit. These thermal properties are quite competitive to the PBT and PBO. The optical absorption spectra are shown in Fig. 6 and the maximum absorption peak λ_{max} summarized in Table III. PBIs synthesized here have λ_{max} comparable to that previously reported and is typically lower than those of PBT and PBO [5, 7]. Similar to thermal analysis, no significant difference can be found among PBI-1 to 3. Substitution of benzyl by naphthalenyl unit in PBI-2 gives almost identical XRD trace (Fig. 6 and Table III). The only difference lies in the longer *c*-axis for PBI-2. Biphenyl substitution of PBI-3 results in a less distinguished (010) peak and a longer *b*-axis ($b = 0.349$ nm). This implies that the biphenyl unit may not line up straight in the *c*-axis direction and the molecule is also less ordered.

The strongly conjugated naphthalene ring apparently offers conjugation by additional π electron, rendering

TABLE III Effect of diacid architecture on the properties of PBIs

Sample	η_{inh} (dL/g)	T_d (°C)	Mass 800°C (wt%)	λ_{max} (nm)	2θ (degree)	*d*-spacing (nm)
PBI-1	2.89	702	81	405	13.276	0.666
					26.139	0.341
PBI-2	2.07	708	85	413	13.128	0.674
					26.067	0.342
PBI-3	2.12	689	83	407	13.249	0.668
					25.533	0.349
PBI-4	1.03	549	18	347	13.539	0.654
					26.889	0.331
PBI-5	2.26	626	50	381	13.155	0.672
					–	–
PBI-6	2.20	509	30	363	13.918	0.636
					–	–

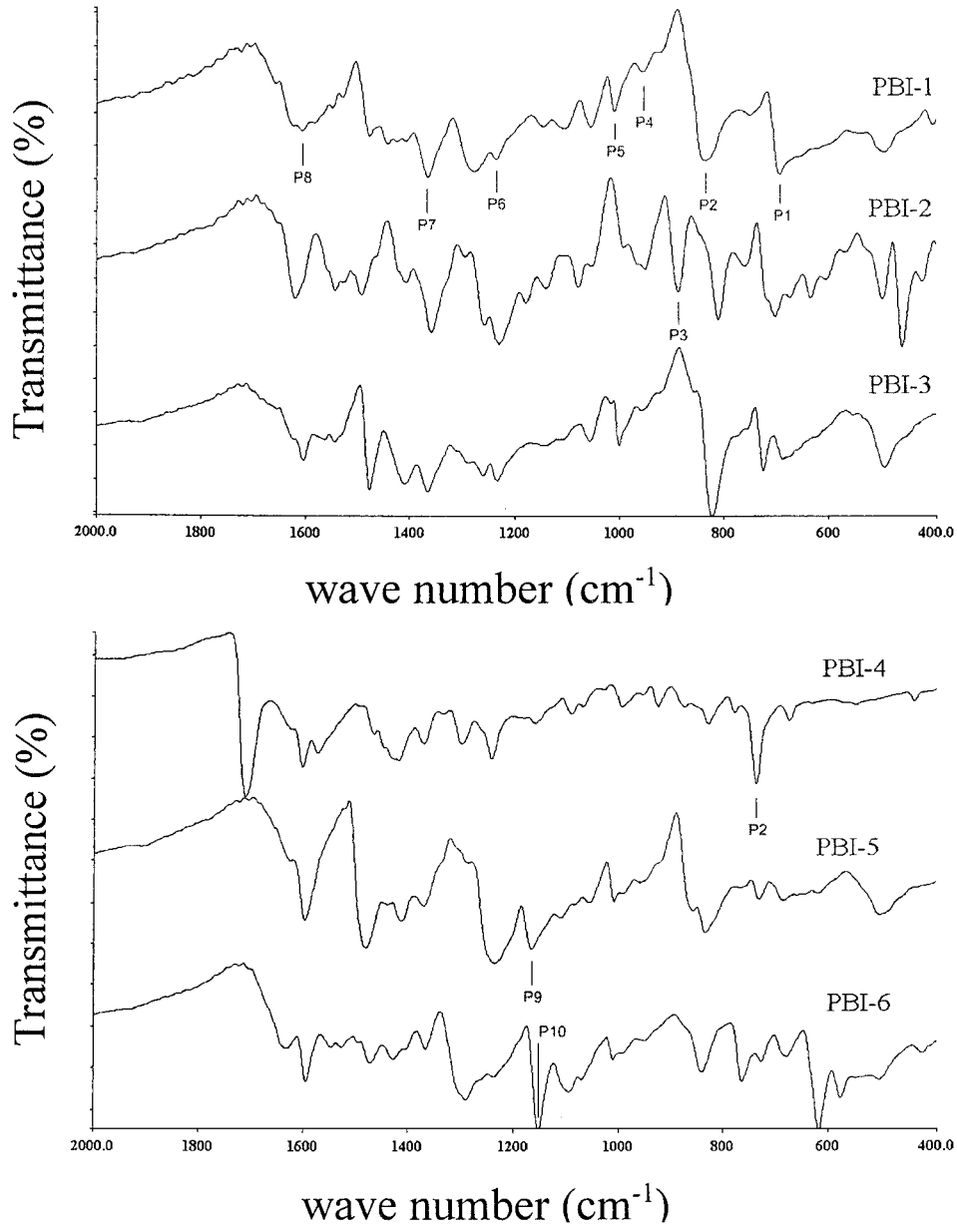

Figure 3 FTIR spectra of six PBIs.

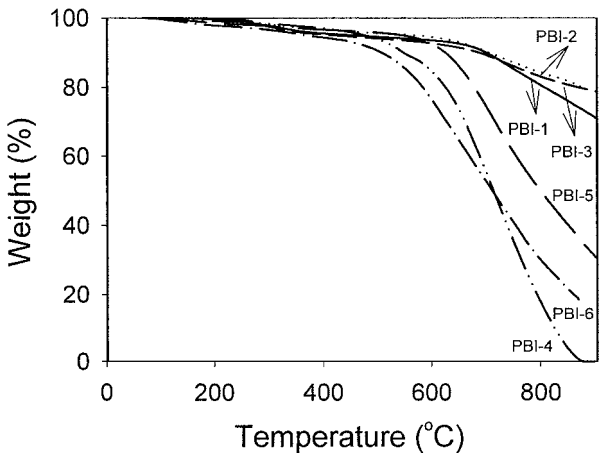

Figure 4 TGA of six PBIs.

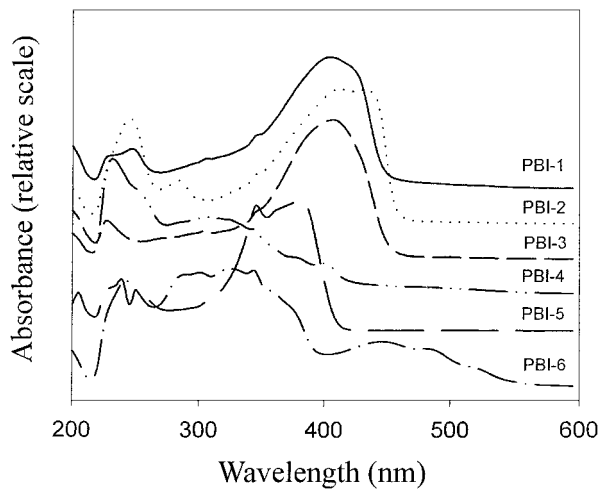

Figure 5 UV-visible absorption spectra of six PBIs.

itself a less confined vibration space, and making also the neighboring heteroring and the C=N bond easier to do resonance stretching and vibration. This resonance effect can be identified from the red shift of PBI-2 by 8 nm in the UV-absorption spectrum (Fig. 5). XRD trace indicates a less compact face-to-face packing of (010) for PBI-3 ($b = 0.349$ nm as compared to 0.341 nm of PBI-1), suggesting a less rigid-rod-like molecular assembly. Thus, there is a strong tendency of coplanarity

TABLE IV Solubility of PBIs

Sample	MSA	DMSO	TFAA	MSA/DCM (80/20 wt%)
PBI-1	++	χ	+	++
PBI-2	++	+	+	++
PBI-3	++	+	+	++
PBI-4	++	+	+	++
PBI-5	++	+	+	++
PBI-6	++	+	+	++

++ = very soluble; + = moderately soluble; χ = insoluble.

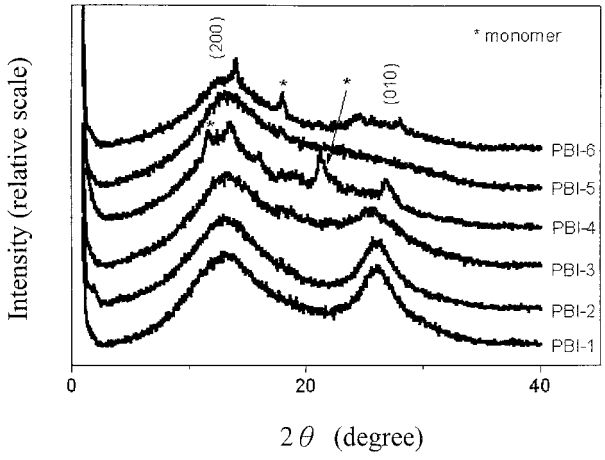

Figure 6 XRD traces of six PBIs.

in the *a*-direction. Although there is no effect on the thermal properties (Table III and Fig. 4), a discernible decrease of η_{inh} in PBI-2 and 3, as compared to PBI-1, is clearly identified. We attribute the latter to the bigger monomer size which results in a more or less retarded polycondensation.

3.4. Symmetry effect

Note that the η_{inh} of PBI-4 is almost half of that of PBI-3 (Table III). FTIR spectra of PBI-3 and PBI-4 show essentially the same bands as that of PBI-1 except for the C_6H_4 ring stretching at a lower frequency, appearing at 824 cm^{-1}, and 736 cm^{-1}, respectively (Fig. 3 and Table IV). This represents a decrease in frequency by 17 cm^{-1} and 105 cm^{-1}, which reflects the strong substitution pattern of the biphenyl ring. Contrary to the naphthalene ring, the biphenyl unit imposes a restriction for free vibration. The asymmetric PBI-4 is thermally very unstable as compared to the symmetrical PBI-3 (Fig. 4 and Table III). This may result from incomplete polycondensation as evidenced from FTIR spectra in Fig. 4 where carboxyl groups─COOH at ~1700 cm^{-1} can be identified. Large "blue shift" of 57 nm can be found for the asymmetric PBI-4 as compared to the symmetrical PBI-3 (Fig. 5 and Table III).

It is interesting to compare the XRD trace of PBI-3 and PBI-4. The molecular order is greatly reduced for the asymmetric PBI-4. The (200) peak splits into two small ones; while (010) peak becomes undetectable (Fig. 6 and Table III). This suggests that molecular structure of PBI-4 is less ordered in the *b*-axis direction due to free rotation between the benzene ring of the biphenyl moiety. Additional minor peaks of monomers spread around further suggest incomplete polymerization. This is attributed to the steric hindrance of the two carboxylic acids.

The asymmetric molecular structure of PBI-4 makes itself more difficult to freely vibrate, yielding a reduced conjugation and coplanarity; thus compared to PBI-3 we observe a great "blue shift" of PBI-4 in the UV-absorption spectra (Table III and Fig. 5). Other effects include a smeared (010) allignment (Fig. 6), a big reduction of molecular weight (>50%, Table III) and worse thermal properties ($T_d < 600°C$, Table III). Yet the (200) alignment is not altered, a strong indication of the coplanarity of PBIs in the *a*-axis direction. Incomplete polymerization of PBI-4 due to asymmetry is another drawback as evidenced by the low η_{inh} and the monomer peaks in XRD trace (Fig. 6 and Table III).

3.5. Solubilization effect

On the other hand, η_{inh} increases, but to a lesser extent, with the incorporation of the "softer" ether or sulfone in the biphenyl unit when comparing PBI-5 and -6 to PBI-3 (Table III). Their FTIR spectra are very similar to that of PBI-1, with the only exception of a lower C═N stretching by ~10 cm^{-1}. Both T_d (76°C and 193°C less) and char yield (31 and 51% less) are greatly reduced as indicated in Table III. The same "blue shift" can also be found (Fig. 5); in addition, the absorption peaks become broader and lower, indicating a larger dispersion of the optical constituent in the PBI molecular structure.

PBI-5 with ether linkage, on the other hands, shows a larger *d*-spacing in the *a*-axis direction ($a = 1.344$ nm, Table III) as compared to PBI-3. Apparently, the flexible oxygen atom allows a looser molecular packing in the *a*-direction. Yet order in the *b*-direction is completely lost as one observes no (010) peak. The same observation can be found for PBI-6, except a shorter *d*-spacing of (002) plane, i.e., $a = 1.272$ nm. This implies a liquid crystal phenomenon in one dimension. However, more experimental evidence is needed to clarify this argument. Distinct scattering peaks of monomers in PBI-6 are also identified, indicative of incomplete polymerization.

The flexible ether and sulfone units were originally designed to improve the solubility of PBX series in organic solvents; This was experimentally proven in Table IV. Compared to the other PBIs, the high molecular weight and rigid-rod PBI-1 makes itself difficult to dissolve in the aprotic organic solvents. Thermal stability is, on the other hand, greatly reduced (Table III). It is apparent that solubility of PBIs in organic solvents is improved but at the expense of a reduced thermal stability. The flexibility and solubility also help to build up a higher molecular weight (Table III).

Yet, problems associated with the electrophilicity by ether and sulfone group can not be ignored. A tremendous "blue shift" in the UV-absorption spectra and a smeared (010) alignment in the XRD (Table III and Figs 5 and 6) can be found. However, it is interesting to note that the (200) spacing is, on the contrary, greatly reduced in the case of sulfonated PBI-6. More experimental evidence is needed to further explain this peculiarity.

4. Conclusions

The synthesis and microstructure of six carefully designed PBIs have been examined in this study. The role of PPA is identified as the solvent, the dehydrochlorinating agent, and the dehydrating agent. Additional phosphorous pentoxide is needed to remove extra water as the polycondensation by-product. Further, the effect of polymer concentration is investigated. It appears that the inherent viscosity or the molecular weight, the decomposition temperature, and the side-to-side molecular packing of PBIs increases with lower polymer concentration. The results are then discussed in terms of the effects of resonance, symmetry, and solubilization of the diacids. For the resonance effect, the strongly conjugated naphthalene ring offers resonance by additional π electron, rendering itself a less confined vibration space, and making also the neighboring heteroring and the C=C bond more easier to do resonance stretching and vibration. This resonance effect can further be identified from the red shift in the UV-absorption spectrum. XRD traces indicate minor change of less than 1% in microstructure in (200) spacing; a less compact face-to-face packing of (010) for PBI-3 is found, suggesting a less rigid-road-like molecular assembly. No significant change on the thermal stability is found. Study on the symmetry effect indicates a decrease of vibration frequency in FTIR and a "blue shift" in UV-visible spectra due to asymmetry. It is also accompanied by a smeared (010) alignment, a large reduction of molecular weight, and worse thermal properties. Introduction of the flexible and electrophilic ether and sulfone linkage results in an improved solubility in organic solvents at the expense of down graded thermal properties. This "electron drawing" effect makes the C=N stretching in the heteroring more difficult; a large "blue shift" in the UV-absorption spectra and a smeared (010) alignment in the XRD thus follow.

Acknowledgements

This work was supported by National Science Council (NSC-88-2218-E-110-001) and by China Petroleum Corporation (NSC-89-CPC-7-110-001). The authors wish to thank Dr. K. S. Lieu at National Chi Nan University for constructive suggestions in the preparation of thin films.

References

1. J. F. WOLFE, in "Encyclopedia of Polymer Science and Engineering," Vol. 11, 2nd ed., edited by H. F. Mark, N. M. Bikales, C. G. Overberger and G. Menges (John Wiley & Sons, Inc., New York, 1988) p. 601.
2. J. F. WOLFE and F. E. ARNOLD, *Macromolecules* **14** (1981) 909.
3. D. B. COTTS and G. C. BERRY, *ibid.* **14** (1981) 930.
4. J. F. WOLFE, B. H. LOO and F. E. ARNOLD, *ibid.* **14** (1981) 915.
5. S. A. JENEKHE, P. O. JOHNSON and A. K. AGRAWAL, *ibid.* **22** (1989) 3216.
6. J. A. OSAHENI and S. A. JENEKHE, *Chem. Mater.* **4** (1992) 1282.
7. S. A. JENEKHE, J. A. OSAHENI and J. S. METH, *ibid.* **4** (1992) 683.
8. J. A. OSAHENI and S. A. JENEKHE, *ibid.* **7** (1995) 672.
9. *Idem.*, *Macromolecules* **28** (1995) 1172.
10. P. A. DEPRRA, J. G. GAUDIELLO and T. J. MARKS, *ibid.* **21** (1988) 2295.
11. S. KIM, D. A. CAMERON, Y. G. LEE, J. R. REYNOLDS and C. R. SAVAGE, *J. Polym. Sci.: Part A: Polym. Chem.* **34** (1996) 481.
12. T. D. DANG, S. J. BAI, D. P. HEBERER, F. E. ARNOLD and R. SPRY, *J. Polym. Sci.: Part B: Polym Phys.* **31** (1993) 1941.
13. M. B. GIESELMAN and J. R. REYNOLD, *Macromolecule* **26** (1993) 5633.
14. R. J. SPRY, M. D. ALEXANDER, JR., S. J. BAI, T. D. DANG, G. E. PRICE, D. R. DEAN, B. KUMAR, J. S. SOLOMON and F. E. ARNOLD, *J. Polym. Sci.: Part B: Polym Phys.* **35** (1997) 2925.
15. L. S. TAN, K. R. SRINIVASAN, S. J. BAI and R. J. SPRY, *J. Polym. Sci.: Part A: Polym. Chem.* **36** (1998) 713.
16. E. W. CHOE and S. N. KIM, *Macromolecules* **14** (1981) 920.
17. S. R. ALLEN, A. G. FILIPPOV, R. J. FARRIS and E. L. THOMAS, *J. Appl. Polym Sci.* **26** (1981) 291.
18. S. J. KRAUSE, T. B. HADDOCK, G. E. PRICE and W. W. ADAMS, *Polymer* **29** (1988) 1959.
19. M. F. ROBERTS and S. A. JENEKHE, *Chem. Mater.* **6** (1994) 135.
20. R. C. EVERS, F. E. ARNOLD and T. E. HELMINIAK, *Macromolecules* **14** (1981) 925.
21. S. C. YU, X. GONG and W. K. CHAN, *ibid.* **31** (1998) 5639.
22. S. A. JENEKHE, P. O. JOHNSON and A. K. AGRAWAL, *ibid.* **22** (1989) 3216.
23. M. F. ROBERTS, S. A. JENEKHE, A. CAMERON, M. McMILLAN and J. PERLSTEIN, *Chem. Mater.* **6** (1994) 658.
24. T. HATTORI, H. AKITA, M. KAKIMOTO and Y. IMAI, *J. Polym. Sci.: Part A: . Polym. Chem.* **30** (1992) 197.
25. *Idem.*, *Macromolecules* **25** (1992) 3351.
26. T. HATTORI, K. KAGAWA, M. KAKIMOTO and Y. IMAI, *ibid.* **26** (1993) 4089.
27. D. S. NELSON and D. S. SOANE, *Polym. Eng. Sci.* **34** (1994) 965.
28. J. W. LEE, C. S. WANG, H. H. SONG and G. E. PRICE, *Polymer* **36** (1995) 955.
29. J. W. LEE, C. S. WANG, G. E. PRICE and D. M. HUSBAND, *ibid.* **38** (1997) 1403.
30. H. H. SONG and S. K. HONG, *ibid.* **38** (1997) 4241.
31. S. J. KRAUSE, T. B. HADDOCK, D. L. VEZIE, P. G. LENHERT, W. F. WANG, G. E. PRICE, T. E. HEMINIAK, J. F. O'BRIEN and W. W. ADAMS, *ibid.* **29** (1988) 1354.

Received 20 November 2001
and accepted 12 June 2002